

# A 1.2V Fully Differential Amplifier with Buffered Reverse Nested Miller and Feedforward Compensations

Meng-Hung Shen, Li-Han Hung and Po-Chiun Huang

Department of Electrical Engineering  
National Tsing Hua University, Hsinchu 30013, Taiwan  
Contact Email: mhshen@larc.ee.nthu.edu.tw

**Abstract**— This paper presents a low voltage CMOS fully differential operational amplifier. It comprises three gain stages with two compensation schemes, buffered reverse nested Miller compensation (B-RNMC) and feedforward transconductance compensation (FFTC). In B-RNMC, a transconductance stage is inserted in the feedback path to eliminate the right half plane (RHP) zero which may degrade phase margin. In FFTC, a feedforward transconductance helps to enhance output large signal response.

Using standard 0.35- $\mu\text{m}$  CMOS technology, measurement results demonstrate that DC gain greater than 90dB, gain-bandwidth product of 8.9MHz, and phase margin of 86° is achieved with 100pF output loads. The settling time for a 1.2V<sub>pp</sub> step is 2.4 $\mu\text{s}$ . All the circuits dissipate 342 $\mu\text{W}$  under a single 1.2V power supply.

## I. INTRODUCTION

An amplifier with large gain, high dynamic range, and wide bandwidth is indispensable in most analog circuits. As the technology scales down to deep submicron, supply voltage decreases with the same extent for reliability issue. Under low supply voltage, traditional approach of cascoding gain stage is not feasible. Therefore, more circuit designers are aware of the multi-stage amplifier design. Stability, however, becomes an important issue as a multi-stage amplifier induces more low frequency poles than a two-stage alternative does. Hence a multi-stage amplifier must be properly compensated to cancel or shift the nondominant poles and zeros to high frequency. Nested Miller compensation (NMC) is a well-known compensation technique for the multi-stage amplifier. It uses multiple feedback loops to assign each pole/zero location. Though NMC scheme provides good stability, it suffers from severe bandwidth reduction and large power dissipation, as mentioned in [1].

To overcome the limitations of NMC, especially when driving heavy capacitive loads, the reversed nested Miller compensation (RNMC) is proposed [2]. Compared to NMC, RNMC exhibits broader bandwidth as the inner compensation loop is not connected to the large capacitors at output. However, it still suffers from right half plane (RHP) zero that degrades the phase margin. To remove the RHP zero, several methods have been proposed [3] [4]. In this paper, the buffered reversed nested Miller compensation is used to extend the amplifier bandwidth. A buffer composed of a transconductance

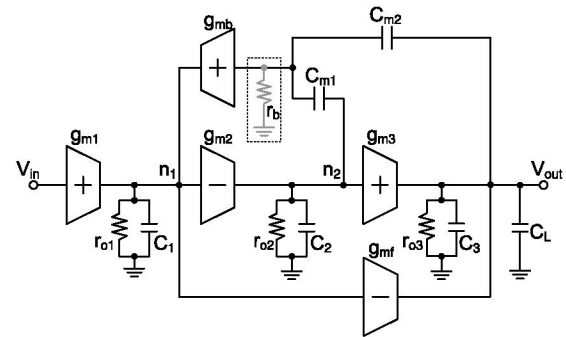


Fig. 1. Block diagram of the amplifier with B-RNMC and FFTC.

stage is connected in series with compensation capacitors. In addition, a parallel feedforward transconductance widely used in either zero location movement or slew rate enhancement is applied in this design to improve small and large signal performance.

This paper is organized as follows. The operating principle and the small-signal analysis of the proposed amplifier are discussed in Section II. Section III and Section IV show the detailed circuit implementation and measurement results, respectively. Finally a conclusion is given in Section V.

## II. CIRCUIT ARCHITECTURE

The block diagram of the proposed topology is shown in Fig. 1. A conventional three stage amplifier consists of three transconductance stages  $g_{m1}$ - $g_{m3}$ . Parameters  $r_{oi}$  and  $C_i$  ( $i=1-3$ ) represent the output resistance and the lumped parasitic capacitance of  $i$ th stage. The feedforward stage,  $g_{mf}$ , along with  $g_{m3}$  forms the output push pull stage to improve the slew rate. A buffer stage  $g_{mb}$  is inserted between the common end of two Miller capacitors  $C_{m1}$  and  $C_{m2}$  and the output of the  $g_{m1}$  stage. It helps to break the feedthrough path from input to output. Thus the RHP zero is eliminated.

### A. Transfer function

Before deriving the small-signal transfer function of the proposed amplifier, some assumptions are made for simplicity:

$$g_{m1}r_{o1}, g_{m2}r_{o2}, g_{m3}r_{o3} \gg 1$$

$$C_L, C_{m1}, C_{m2} \gg C_{1-3}.$$

The input impedance of the buffer stage is modeled as  $r_b$ , which can be presumed:

$$r_b = \frac{1}{g_{mb}}. \quad (1)$$

Neglecting second order terms, the open loop gain of the circuit shown in Fig. 1 is given by the following equation:

$$A(s) = -\frac{A_{dc}(1 + \frac{s}{\omega_3} + \frac{s^2}{\omega_4})}{(1 + \frac{s}{\omega_{P1}})(1 + \frac{s}{\omega_1})(1 + \frac{s}{\omega_2})} \quad (2)$$

where

$$A_{dc} = g_{m1}r_{o1}g_{m2}r_{o2}g_{m3}r_{o3} \quad (3)$$

$$\omega_1 = \frac{g_{m2}g_{m3}C_{m2}}{C_{m1}(g_{mf}C_{m2} + g_{m2}(C_{m2} + C_L))} \quad (4)$$

$$\omega_2 = \frac{g_{mb}r_{o1}(g_{mf}C_{m2} + g_{m2}(C_{m2} + C_L))}{C_{m2}C_L} \quad (5)$$

$$\omega_3 = \frac{g_{m2}g_{m3}g_{mb}}{g_{mf}g_{mb}C_{m1} + g_{m2}g_{m3}(C_{m1} + C_{m2})} \quad (6)$$

$$\omega_4 = \frac{g_{m2}g_{m3}g_{mb}}{(g_{m2} + g_{mf})C_{m1}C_{m2}}. \quad (7)$$

Due to Miller effect,  $C_{m2}$  is amplified by the last two gain stage. So the dominant pole is located at

$$\omega_{P1} \approx \frac{1}{r_{o1}A_2A_3C_{m2}} = \frac{1}{r_{o1}g_{m2}r_{o2}g_{m3}r_{o3}C_{m2}}. \quad (8)$$

The gain-bandwidth product can be expressed as

$$\omega_0 = 2\pi \cdot GBW = A_{dc} \cdot \omega_{P1} = \frac{g_{m1}}{C_{m2}}. \quad (9)$$

Because the coefficients of  $s$  and  $s^2$  in the numerator are both positive, two zeros are located at left half plane (LHP). Furthermore, the transconductance of last two stages,  $g_{m2}$  and  $g_{m3}$ , can be reduced since  $g_{mb}$  provides additional gain in feedback loops. Therefore, smaller power consumption is expectable.

Generally  $r_b$  is small. If the feedforward stage transconductance  $g_{mf}$  is neglected, the transfer function (2) can be simplified as

$$A(s) = -\frac{A_{dc}}{(1 + \frac{s}{\omega_{P1}})[1 + \frac{C_{m1}(C_{m2} + C_L)}{g_{m3}C_{m2}}s]}. \quad (10)$$

The phase margin is

$$PM \approx \tan^{-1}\left(\frac{g_{m3}}{g_{m1}} \frac{C_{m2}^2}{C_{m1}(C_{m2} + C_L)}\right). \quad (11)$$

Once  $C_{m2}$  is decided by the required unity gain bandwidth, and  $g_{m1}$ ,  $g_{m3}$  and  $C_L$  are already known, the phase margin can be solely determined by selecting  $C_{m1}$  adequately [3].

### B. System estimator

To estimate the system parameters efficiently, a tool based on Matlab is developed. The kernel of this tool is a symbolic analyzer [5]. According to Kirchhoff's voltage and current laws, the matrix between each node voltage and branch current is firstly constructed. Then the output to input symbolic

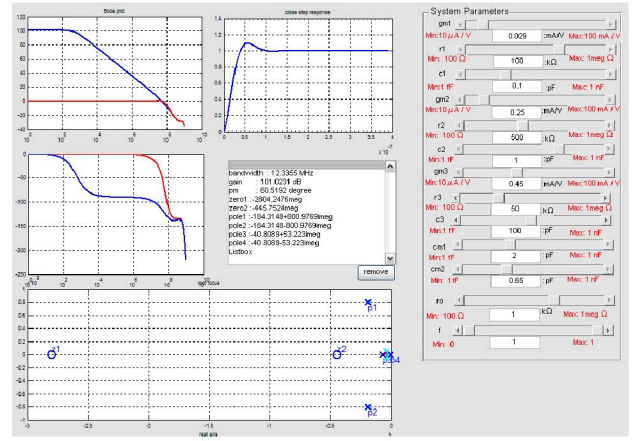


Fig. 2. System estimation platform.

transfer function can be solved with the assistance of Matlab routines. The symbolic analysis is much more precise than simplified equations from hand calculation. The main problem of the symbolic analysis is the computation complexity. For example, the transfer function of the proposed amplifier contains three poles and two zeros. Each coefficient contains a complicated combination of different component values. For ease of usage, we developed a user-friendly interface, as shown in Fig. 2. Designers can enter each parameter of the amplifier, then the frequency response, settling behavior, pole/zero locations and root locus come out in the main window. In addition, the performance difference can be easily observed by altering the parameters. With the aid of this tool, designers can estimate the system performance quickly and precisely.

## III. CIRCUIT IMPLEMENTATION

The schematic of the three stage fully differential amplifier is shown in Fig. 3. First stage composed of  $M_{11}$ - $M_{16}$  is a classical folded cascode OTA, which has a wide input common mode range and large output impedance. A simple common source amplifier,  $M_{21}$  and  $M_{22}$ , is adopted as the second stage. To attain fast time domain response, a push pull output stage is accomplished by  $M_{31}$ - $M_{34}$  to enhance slewing in both charging and sinking directions. The buffer stage  $g_{mb}$  comprising  $M_{c2}$  blocks the high frequency signal path from drain of  $M_{16}$  to output node through  $C_{m2}$ .

For a fully differential amplifier, a common mode feedback (CMFB) circuit is necessary to set up the common mode voltage of the two output nodes. To attain maximum output swing, the output voltage should be at the half of supply voltage, that is 0.6V in this work. Unfortunately, this voltage level is too small to turn on neither P nor N-type transistor of the technology we used. A current compared CMFB circuit, as depicted in Fig. 4, is used to solve this problem [6]. This topology transfers the output voltages to a common mode current by  $2R$  resistors. The current is then compared with a reference current generated by  $V_{ocm}$  to produce the CMFB voltage  $V_{cmc}$ .  $V_{cmc}$  is connected to the gate of  $M_{14}$  to form

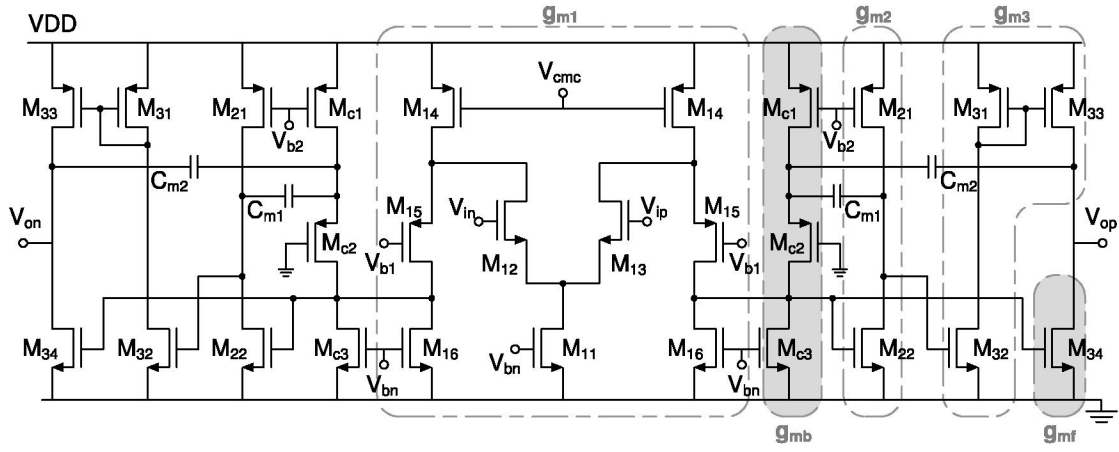


Fig. 3. Schematic of the proposed fully differential amplifier.

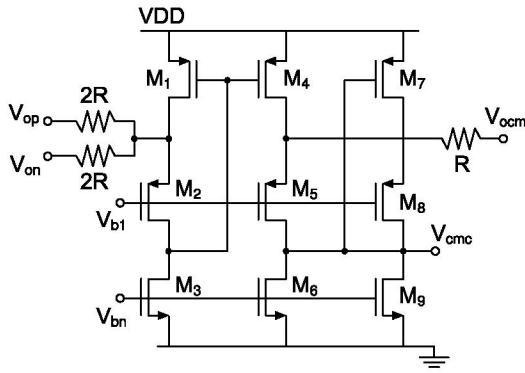


Fig. 4. Current compared CMFB circuit.

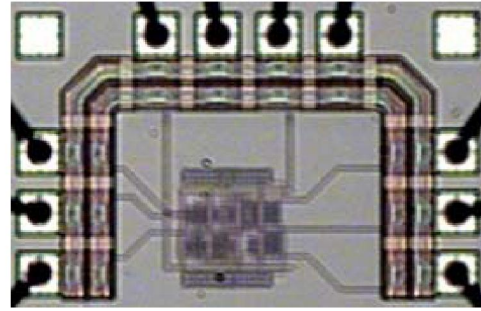


Fig. 5. Microphotograph of the test chip.

the feedback loop. The gain of this CMFB loop is decided by the current sensing resistor and the transconductance of  $M_7$ , which is  $A_{CMFB} = (g_{m7} \cdot R)^{-1}$ .

#### IV. MEASUREMENT RESULTS

Fig. 5 shows the chip microphotograph. It uses 0.35- $\mu\text{m}$  double poly four metal CMOS technology. Under a 1.2V supply and 100pF output capacitance loads, the open loop frequency response is shown in Fig. 6. The unity gain frequency is 8.9MHz and phase margin is 86°.

To maximize the signal swing, the input dc voltage is normally set at  $V_{DD}/2$ . However, this voltage level is not large enough to turn on any transistor in our case. As illustrated in Fig. 7, the low voltage bias scheme for close loop measurement is adopted to solve this problem [6]. Since input common mode voltage has to be greater than  $V_{TN} + V_{DSSat,12} + V_{DSSat,11}$ , operating points of  $V_{ip}$  and  $V_{in}$  are chosen as 0.75V. Two bias resistors  $R_b$  are connected to provide dc setup current required by  $R_i$  and  $R_f$ .

The measured transient response is shown in Fig. 8. Slew rate under a 1.2V step signal is 5.5V/ $\mu\text{s}$  and the settling time to 1% is 2.4 $\mu\text{s}$ . For a 100kHz 1V<sub>pp</sub> input signal,  $HD_3$  of this test chip is below -70dB. Total power dissipation is 342 $\mu\text{W}$

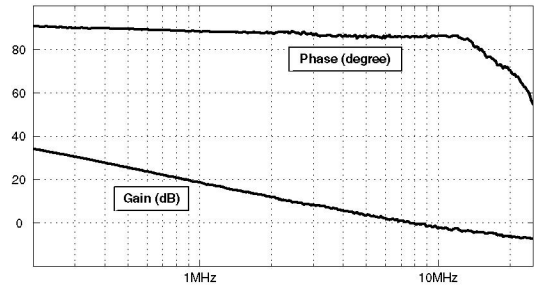


Fig. 6. Measured open loop ac response.

TABLE I  
MEASUREMENT RESULTS

$C_L$	100pF	$A_{dc}$	>90dB
GBW	8.9MHz	Phase Margin	86°
$V_{dd}$	1.2V	$I_{dd}$	0.285mA
Power	0.342mW	THD	<-70dB
Slew Rate	5.5V/ $\mu\text{s}$	Settling Time	2.4 $\mu\text{s}$

under a single 1.2V power supply. Table I summarizes the measurement results.

The summary of the performance of different amplifiers in the literature is given in Table II. The comparison between

TABLE II  
PERFORMANCE COMPARISON OF DIFFERENT COMPENSATION TOPOLOGY

		$C_L$ (pF)	Vdd (V)	Idd (mA)	Power (mW)	GBW (MHz)	SR (V/ $\mu$ s)	$FOM_S$ ( $\frac{GBW \cdot C_L}{Power}$ )	$FOM_L$ ( $\frac{SR \cdot C_L}{Power}$ )
NMC	[1]	100	8.0	9.5	76	60	20	79	26
RNMCR	[4]	15	3.0	0.467	1.4	19.46	11.1	209	119
GFPC	[7]	300	3.0	0.817	2.45	10.4	3.5	1273	469
AFFC	[8]	120	2.0	0.20	0.40	4.5	1.49	1350	447
DLPC	[9]	120	1.5	0.22	0.33	7.0	3.3	2545	1200
ACBC	[10]	500	2.0	0.162	0.324	1.90	1.0	2932	1543
TCFC	[11]	150	1.5	0.03	0.045	2.85	1.03	9500	3450
This Work		100	1.2	0.130*	0.156*	8.9	5.5	5705	3526

\* equivalent case as all the amplifiers are with single ended output.

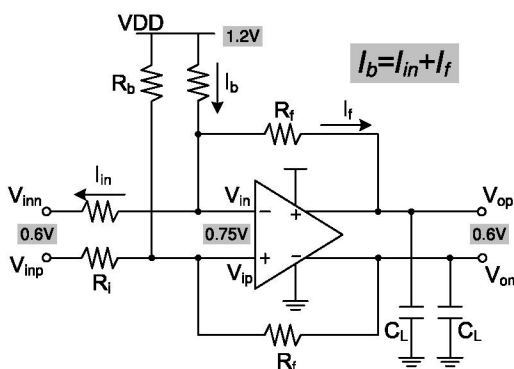


Fig. 7. Close loop bias scheme.

different compensation topologies is based on two figures of merits,  $FOM_S$  and  $FOM_L$  [11]. To make fair comparisons, current and power consumption of our work are reconfigured as the single-ended case. Our work exhibits competitive performance in both small-signal bandwidth and large-signal slew rate.

## V. CONCLUSION

In this paper, a parallel of buffered reverse nested Miller and feedforward transconductance compensations is introduced. Based on this topology, a 1.2V CMOS fully differential amplifier, including a current compared common mode feedback circuit, has been successfully verified with silicon. Apart from that, a symbolic estimator with a user-friendly interface is developed to precisely analyze high order system. This work exhibits remarkable performance either in small signal bandwidth or large signal behavior compared with other compensation topologies.

## ACKNOWLEDGMENT

The authors would like to express their gratitude to National Chip Implementation Center (CIC) for chip fabrication support.

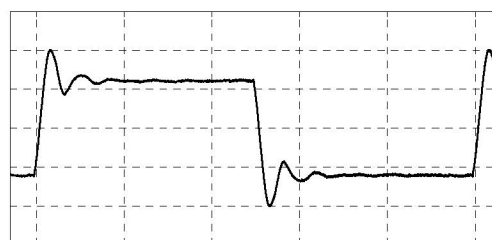


Fig. 8. Measured pulse response for large input signal.(Xdiv:2 $\mu$ S. Ydiv:0.5V)

## REFERENCES

- [1] R. Eschanzier, L. Kerklaan, and J. Huijsing, "A 100-MHz 100-dB operational amplifier with multipath nested miller compensation structure," *IEEE J. Solid-State Circuits*, vol. 27, no. 12, pp. 1709–1717, Dec. 1992.
- [2] R. Eschanzier and J. Huijsing, *Frequency Compensation Techniques for Low-Power Operational Amplifier*. Kluwer Academic Publishers, 1995.
- [3] R. Mita, G. Palumbo, and S. Pennisi, "Design guidelines for reversed nested miller compensation in three-stage amplifiers," *IEEE Trans. Circuits Syst. II*, vol. 50, no. 5, pp. 227–233, May 2003.
- [4] K. P. Ho, C. F. Chan, C. S. Choy, and K. P. Pun, "Reversed nested miller compensation with voltage buffer and nulling resistor," *IEEE J. Solid-State Circuits*, vol. 38, no. 10, pp. 1735–1738, Oct. 2003.
- [5] G. Gielen, P. Wambacq, and W. Sansen, "Symbolic analysis methods and applications for analog circuits: A tutorial overview," *Proc. of the IEEE*, vol. 82, no. 2, pp. 287–304, Feb. 1994.
- [6] S. Karthikeyan, S. Morteza pour, A. Tammineedi, and E. Lee, "Low-voltage analog circuit design based on biased inverting opamp configuration," *IEEE Trans. Circuits Syst. II*, vol. 47, no. 3, pp. 176–184, Mar. 2000.
- [7] P. K. Chan and Y. C. Chen, "Gain enhanced feedforward compensation technique for pole-zero cancellation at heavy capacitive load," *IEEE Trans. Circuits Syst.*, no. 50, pp. 933–941, Dec. 2003.
- [8] H. Lee and P. K. T. Mok, "Active-feedback frequency-compensation technique for low-power multistage amplifiers," *IEEE J. Solid-State Circuits*, vol. 38, no. 3, pp. 511–520, Mar. 2003.
- [9] H. Lee, K. N. Leung, and P. K. T. Mok, "A dual-path bandwidth extension amplifier topology with dual-loop parallel compensation," *IEEE J. Solid-State Circuits*, vol. 38, no. 10, pp. 1739–1744, Oct. 2003.
- [10] X. Peng and W. Sansen, "Ac boosting compensation scheme for low-power multistage amplifiers," *IEEE J. Solid-State Circuits*, vol. 39, no. 11, pp. 2074–2079, Nov. 2004.
- [11] —, "Transconductance with capacitances feedback compensation for multistage amplifiers," *IEEE J. Solid-State Circuits*, vol. 40, no. 7, pp. 1514–1520, July 2005.